Title
Simulations of Silicon Vertex Tracker for Star Experiment at RHIC (RD-22)

Permalink
https://escholarship.org/uc/item/6563x3pf

Authors
Odyniec, G.J.
Cebra, D.
Christie, W.
et al.

Publication Date
1992

LBL-31773

Lawrence Berkeley Laboratory
UNIVERSITY OF CALIFORNIA

Presented at the RHIC R&D Symposium, Brookhaven National Laboratory, Upton, NY, October 10–11, 1991, and to be published in the Proceedings

Simulations of Silicon Vertex Tracker for STAR Experiment at RHIC (RD-22)

G. Odyniec, D. Cebra, W. Christie, D. Liko, S. Margetis,
C. Naudet, L. Schroeder, W. Wilson, J. Cramer,
D. Prindle, T. Trainor, and W. Braithwaite

January 1992

NUCLEAR SCIENCE DIVISION

Prepared for the U.S. Department of Energy under Contract Number DE-AC03-76SF00098

LBL-31773

Presented at RHIC R&D Symposium,
Brookhaven National Laboratory, Upton, New York, USA
10-11 October 1991, and to be published in the Proceedings

SIMULATIONS OF SILICON VERTEX TRACKER FOR STAR EXPERIMENT AT RHIC (RD-22)

G. Odyniec, D. Cebra, W. Christie, D. Liko*, S. Margetis**, C. Naudet,
L. Schroeder, W. Wilson
Nuclear Science Division, Lawrence Berkeley Laboratory
University of California, Berkeley, CA 94720

J. Cramer, D. Prindle, T. Trainor, W. Braithwaite***
University of Washington
Seattle, WA 98195

* Institut fur Hochenenergiephysik, Vienna, Austria
** University of Frankfurt, Frankfurt, Germany
*** University of Arkansas, Little Rock, AR

January 1992

This work was supported by the Director, Office of Energy Research, Division of Nuclear Physics of the Office of High Energy and Nuclear Physics of the U.S. Department of Energy under Contract DE-AC03-76SF00098

SIMULATIONS OF SILICON VERTEX TRACKER FOR STAR EXPERIMENT AT RHIC (RD-22)

G.Odyniec, D.Cebra, W.Christie, D.Liko*, S.Margetis**, C.Naudet,
L.Schroeder, W.Wilson
Lawrence Berkeley Laboratory,
Berkeley, CA 94720

J.Cramer, D.Prindle, T.Trainor, W.Braithwaite***
University of Washington,
Seattle, WA 98195

ABSTRACT

The first computer simulations to optimize the Silicon Vertex Tracker (SVT) designed for the STAR experiment at RHIC are presented.

1.INTRODUCTION

The physics goals [1,2] and the expected complexity of the events at RHIC dictate the design of a tracking system for the STAR experiment. The proposed tracking system will consist of a silicon vertex tracker (SVT) to locate the primary interaction and secondary decay vertices and to improve the momentum resolution, and a time projection chamber (TPC), positioned inside a solenoidal magnet, for

---

* Institut fur Hochenenergiephysik, Vienna, Austria.

** University of Frankfurt, Frankfurt, Germany.

*** University of Arkansas, Little Rock, AR continuous tracking, high momentum resolution, and particle identification. The extremely high position resolution required of the SVT detector is particularly important for the measurement of strangeness and charm production.

However, it must be noted that, although the strange quark density in the quark-gluon plasma phase is much higher than in the hadronic gas phase, the total content of strange quarks is less enhanced in a quark-gluon plasma than in a fully equilibrated hadronic gas at constant total energy or entropy. This is because the volume associated with the hadronic gas is much larger due to the smaller number of available degrees of freedom at fixed energy [3]. Therefore, the observables which depend on the total strangeness abundance, such as Λ, Λ, K^0 yields or K/π ratio should not be considered as direct signatures of quark-gluon plasma formation. On the other hand, the observables depending on enhanced strangeness density, such as baryons with multiple strangeness or possibly correlations between strange particles, benefit from higher (near equilibrium) strangeness density reached in the quark-gluon plasma. Their relative independence of final state effects makes them much more characteristic signatures of quark-gluon plasma formation [4]. The STAR SVT, with its excellent vertexing, will allow for studying multistrange baryon production at RHIC.

It has been argued [5] that the enhancement of the final total open charm, which is mainly due to pre-equilibrium production, could be used as a measure of the thermalization time of the dense partonic system. The SVT capability of open charm detection is currently under investigation.

During FY'91 simulations of SVT performance in the high multiplicity environment at RHIC have been carried out in collaboration with the University of Washington. The goal was to obtain an initial SVT design.

This note is divided into 8 sections. The second section contains a brief description of the detector layout. The third section explains the simulation procedure and lists the various hit densities for central Au+Au FRITIOF events. Sections 4 and 5 deal with reconstruction of primary and secondary verticies. Section 6 describes the effectivness of the SVT-TPC matching algorithm and possible improvements. Section 7 is devoted to Kalman filtering and presents some preliminary results. Finally, section 8 contains a summary.

2. SVT LAYOUT

Fig.1 shows the STAR experimental configuration with the SVT placed in the center of the detector. Fig.2 shows SVT layout presently used in the simulations.

Individual detectors are grouped into ladders. Each ladder holds a row of 6 silicon drift detectors (SDD). The ladders are arranged in three concentric barrels around the interaction at radii of 5, 8, and 11 cm (containing approximately 36K channels of information). Each barrel is about 40 cm in length, to nearly cover the diamond size. Each SDD is 6.5 cm in length and is made from a 4-inch diameter wafer. The thickness of a wafer is 300 microns which appears to be a good compromise between signal strength (24K electrons are created by minimum ionizing particle) and acceptable values of multiple scattering and secondary particle production for particles traversing the detector. Choice of SDD as the basic component of the SVT system was dictated by the excellent performance of these detectors, in particular: outstanding tracking precision (~10 microns), very good two-track resolution (few hundred microns), no dead time, low number of electronic channels, and the ability to monitor and calibrate the system [6,7,8].

3. SIMULATION PROCEDURE

The FRITIOF event generator was used to create Au+Au central events at E_{beam} = 100 GeV/N. The events were then filtered through the STAR detector systems using GEANT. The spatial resolution used in simulations was σ=25 microns for SVT and σ=250 microns for TPC. Interactions with all materials in the present STAR design were taken into account. Multiple scattering, energy loss, secondary interactions, and all other physics processes in GEANT were included.

A typical central Au+Au FRITIOF event at RHIC energies gives rise to about 2900 charged particles that leave at least 20 hits in the TPC. There are about 2400 hits in SVT layer 3 (at 11 cm), 2800 hits in layer 2 (at 8 cm) and 3600 hits in layer 1 (at 5 cm). The average hit densities are 0.71 hits/cm^2, 1.2 hits/cm^2 and 2.3 hits/cm^2 in layer 3, layer 2 and layer 1, repectively.

4. MAIN VERTEX

Fig.3 shows the capability of locating the primary vertex along the beam axis (z axis) with and without the SVT. Tracks can be associated with their correct vertex from events whose vertices are separated by 2 mm, as seen in Fig.3b. The precision of finding the main vertex position in the perpendicular directions (x and y) is significantly better than along the beam axis.

5. SECONDARY VERTICES

5.1 Singly strange particles: K^0, Λ, $\bar{\Lambda}$

The K^0, Λ and $\bar{\Lambda}$ produced in FRITIOF Au+Au events were used to evaluate the efficiency of detection of neutral strange particles decays. About 25% of K^0 and 20% of Λ and $\bar{\Lambda}$ are within the overall detector acceptance. The majority of losses are due to non-charge decays and the acceptance of STAR. To reduce the high density of potential crossing tracks near the primary vertex, a minimum track length of 1 cm for K^0 and 2 cm for Λ and $\bar{\Lambda}$ was applied (this is in effect a lifetime cut). In addition, the parent particle reconstructed from the two secondaries ($K^0 \rightarrow \pi^+ + \pi^-$, $\Lambda \rightarrow p + \pi^-$, $\bar{\Lambda} \rightarrow \bar{p} + \pi^+$) was required to point back to the primary vertex within 2 mm. Fig.4 shows the effective mass distributions for reconstructed events. Sharp peaks at the correct masses are obtained above a flat background. Approximately 2/3 of the accepted secondary neutral decays are reconstructed.

5.2 Charged Hyperons : Ξ^-, Ω^-

Among the multistrange particles only $\Xi^- \rightarrow \pi^- + \Lambda$ and $\Omega^- \rightarrow K^- + \Lambda$ decays can be studied at STAR. The 15000 Ξ's (+ 13000 $\bar{\Xi}$'s) and 300 Ω's (+300 $\bar{\Omega}$'s) produced in 4000 FRITIOF Au+Au events were analyzed. Note that the considered Ξ and Ω decays have the same topology, as shown on Fig.5. As a consequence of the very short lifetime (down to 10^{-13} s), the decaying particle track is straight and its momentum cannot be determined. A 3 constraint fit (3C) with the assumed mass of the decaying particle, or a 2 constraint (2C) fit with the mass calculated must be performed. All measured quantities (e.g. for $\Omega^- \rightarrow K^- +$ Λ; momenta of K^- and Λ) are then fitted to give the best solution [9] and the probability for the correctness of the hypothesis is calculated. To optimize the signal to background ratio, a number of cuts were imposed (analogous to those for Λ, $\overline{\Lambda}$ and K^0): tracks which miss the main vertex by less than 2 cm for Ξ's and 1 cm for Ω's were excluded, a reconstructed hyperon was required to point back to the main vertex within 1.5 mm, and the distance of closest approach for the Λ decay products in all three directions should not exceed 5 mm. Overall about 15% of multistrange baryons which were within STAR acceptance were reconstructed (which corresponds to ~5.5 % of all Ξ's, $\overline{\Xi}$'s, Ω's and $\overline{\Omega}$'s produced produced in full phase space). The bulk of the losses (~ 85%) are due to the limited acceptance of STAR and, for Ω's, due to the branching ratio (67% for $\Omega^- \rightarrow K^- + \Lambda$). Fig.6 a and b show the invariant mass distribution ('ideal' case, without accounting for momentum resolution) for Ξ's reconstructed in STAR TPC (a) alone and TPC with the SVT (b). The SVT eliminated the background almost completely, whereas TPC alone could only provide marginal information on Ξ production, even in the so called 'ideal' case with the perfect momentum measurements. Fig. 7 shows the invariant mass of Ξ (TPC + SVT) for a TPC momentum resolution of $\delta p/p=1\%$ taken to the account. The peak is slightly broader, but the signal is still very strong (note: different vertical scales on Fig. 6 and 7).The arrows indicate the correct masses of hyperons.

Similar results were obtained for $\overline{\Xi}$'s, Ω's and $\overline{\Omega}$'s. As an example, the invariant mass plot for omegas is shown on Fig.8.

6. MATCHING SVT HITS WITH TPC TRACKS

The results of the previous sections were based on the assumption that a perfect assignment of SVT hits with tracks identified in the TPC was possible. An algorithm to examine how well this assignment can be justified was developed. Au+Au events, generated by FRITIOF, were used as described before. A track was required to have 20 points left in the TPC to ensure good tracking information, and three SVT hits (do not confuse acceptance with matching efficiency). A helix was fitted to 20 GEANT points and its parameters were used to calculate the expected hit position in SVT layer 3. The expected multiple scattering of the track was calculated and used to define a 3σ 'search' area. The deviation between the expected position and the actual position is well described by multiple scattering calculation and the chosen 3σ area contain the correct hit over 98 % of the time. Over one third of the time there is only one hit in the search area. All candidates in layer 3 were tested by adding them (one at a time) to the TPC points and re-doing the helix fit. Using the improved helix parameters, extrapolation to the layer 2 was made, and subsequently to the SVT layer 1.

After this procedure, sets of three candidate points for each track were found. Normally there is only one possible helix. When there is more than one helix the one with the lowest χ^2 was chosen. The helix is defined as being 'correct' when all three SVT points and the TPC points come from the same GEANT track. A measure how well matching is done is expressed by ratio of 'correct' helices to the number of times the attempt to find the track was made. This efficiency as a function of p_t is plotted in Fig.9. The overall average efficiency, for a p_t cutoff at 100 MeV/c, is 91%. For p_t cutoff of 200 MeV/c matching efficiency is over 97%.

For tracks with lower p_t there are serious problems with multiple scattering. There are two obvious software improvements to make. The first is the use of KALMAN filter techniques. The second is to assign the tracks to a vertex and use this as a constraint. Regardless of software optimizations, FRITIOF predicts a significant number of tracks at low enough p_t such that the track parameters are altered before they are measured in the TPC. To make the SVT-TPC match for low p_t tracks one would need to start tracking in the TPC closer than 50 cm or add a 4-th layer to the SVT at ~ 20 cm radius. Conversely, one could use the SVT information alone to determine the track parameters of these tracks. Adding a fourth layer to the SVT would make the device an independent tracker for low p_t particles and enlarge the STAR acceptance significantly. This problem is currently under study.

7. KALMAN FILTER METHOD

The Kalman Filter, a method derived from system theory, has been recently proposed as a novel approach to the reconstruction of charged tracks and vertex fitting [10].

Concerning the reconstruction of charged tracks - it combines the advantages of the former methods, especially if the tracks are fitted with breakpoints [11], and adds a new concept for identification of outliers[12].

The vertex fit by means of the Kalman Filter is equivalent to traditional methods based on LSM estimators. However, an advantage is gained by an easy and fast method of outlier identification that allows reconstruction of a primary vertex in the presence of a large number of tracks.

The Kalman Filter method was implemented for the purpose of reconstructing charged tracks with the STAR SVT and TPC. Results from the comparison of the performance of the TPC alone and the TPC combined with the SVT are shown on Fig.10, 11, and 12. Fig.10 shows the momentum resolution obtained in the STAR TPC. Adding the SVT hits improves resolution significantly. The impact parameter resolution (accuracy of extrapolation in the vertex region) is dramatically improved. Fig.11 shows the comparison of impact parameters with and without SVT. In Fig.12 the extrapolation is shown as a function of transverse momentum.

Implementation of the Kalman Filter method to include the primary vertex fitting is currently in progress. As a next step, a Kalman Filter algorithm is going to be incorporated into a reconstruction of secondary vertices, particularly D^+ and D^- finding.

8. SUMMARY

Our investigations and simulation studies have shown that the STAR SVT, together with the TPC, will identify very well the secondary and primary vertices. The overall track momentum resolution is significantly improved. We conclude that the SVT is the <u>only</u> detector capable of measuring multistrange hyperons at RHIC and perhaps allows the study of open charm production.

References:

1. Kadija at al., "An Experiment on Particle and Jet Production at Midrapidity", LBL-29651.
2. The STAR Collaboration, "Update to the RHIC Letter of Intent for an Experiment on Particle and Jet Production at Midrapidity", LBL-31040.
3. L.McLerran, Nucl.Phys. A461,245c(1987),
   K.Redlich, Z.Physik C27,699(1985)
4. P.Koch,B.Muller,J.Rafelski, Phys.Rep.142,167(1986).
   J.Rafelski,A.Schnabel, "Intersections Between Nuclear and Particle Physics", AIP Proceedings No.176(1988),p.1068 and references therein.
5. B.Muller and X.Wang, Duke University Preprint DUKE-TH-91-29.
   E.V.Shuryak, Phys.Lett.78B(1978)150.
   T.Matsui and H.Satz, Phys.Lett.178B(1986)416.
   A.Shor, Phys.Lett.B215(1988)375 and Phys.Lett.B233(1989)231,
6. P.Rehak et al., NIM A248(1986)367.
7. E.Gatti, P.Rehak and M.Sampietro, NIM A274(1989)469.
8. P.Rehak and E.Gatti, NIM A289(1990)410.
9. B.Ronne, CERN/TC, "Kinematical Analysis".
10. R.Fruhwirth, NIM A262(1987)444.
11. R.Bock, H.Grote, D.Notz and M.Regler (ed. by M.Regler) - Data Analysis Techniques in High Energy Physics Experiments, Cambridge Univ. Press, Cambridge (UK), 1990.
12. R.Fruhwirth, Ph.D. Thesis, Univ. of Technology, Vienna, 1988; HEPHY PUB-516/88.

Figures:

Fig.1 STAR experimental configuration.

Fig.2 SVT layout used in the present simulations.

Fig.3 Primary vertex resolution (along beam direction) using: TPC tracking only (a) and TPC+ SVT tracking (b).

Fig.4 Invariant mass plots for Λ, Λ and K^0 reconstructed from 10 full FRITIOF/GEANT Au+Au events. Shaded areas represent the contribution from random background.

Fig.5 Topology for Ξ and Ω decays.

Fig.6 Invariant mass distributions ('ideal' case) for Ξ's reconstructed in STAR TPC (a) alone and TPC with the SVT (b). Shaded areas represent the contribution from random background.

Fig.7 Invariant mass distribution of Ξ (TPC+SVT) with TPC momentum resolution taken to the account. Shaded areas represent the contribution from random background.

Fig.8 Invariant mass distribution of Ω reconstructed in STAR SVT and TPC. Shaded areas represent the contribution from random background.

Fig.9 Matching efficiency as a function of pt.

Fig.10 Momentum resolution for tracks reconstructed by TPC hits alone and by TPC hits and SVT hits. The same track sample has been used to derive these numbers.

Fig.11 Impact parameter distribution of reconstructed primary tracks. For comparison the impact parameter distribution of secondary tracks is shown in the shaded area.

Fig.12 Extrapolation resolution to the vertex region for tracks reconstructed by TPC hits alone and by TPC hits and SVT hits. The same track sample has been used to derive these numbers.

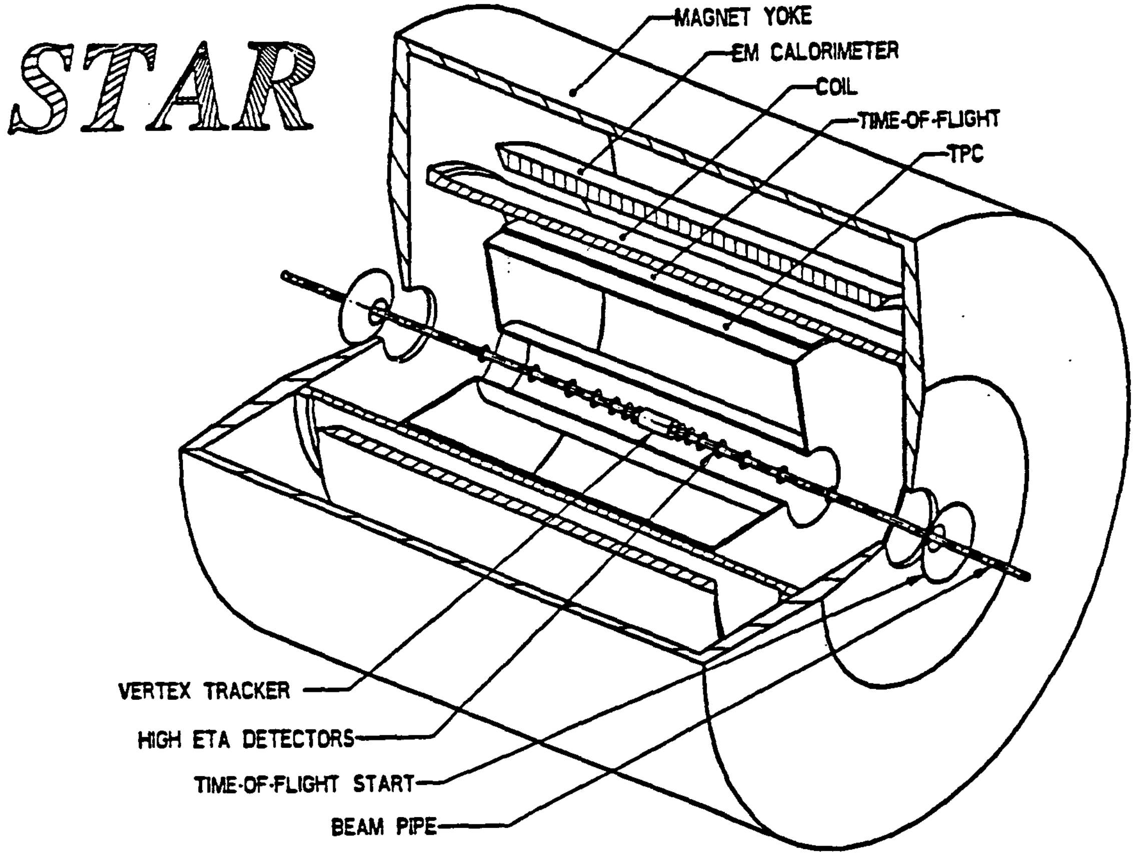

Fig.1 STAR experimental configuration.

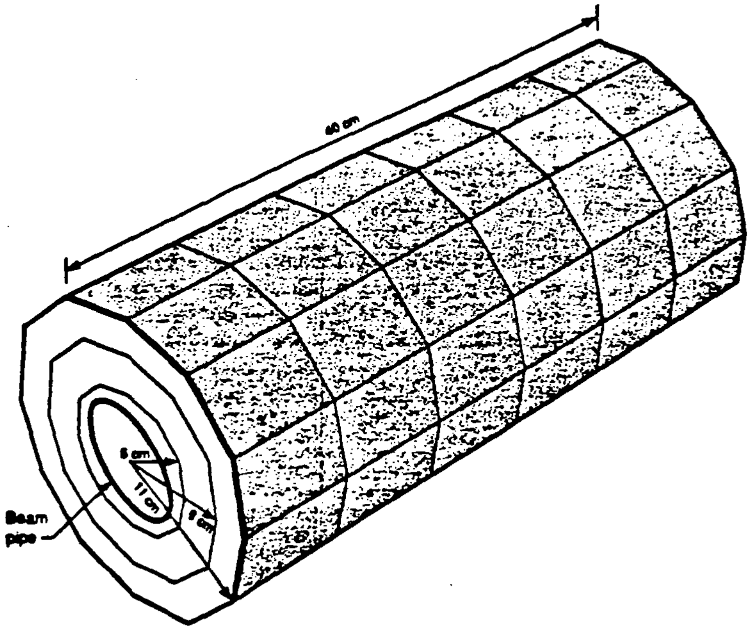

Fig.2 SVT layout used in the present simulations.

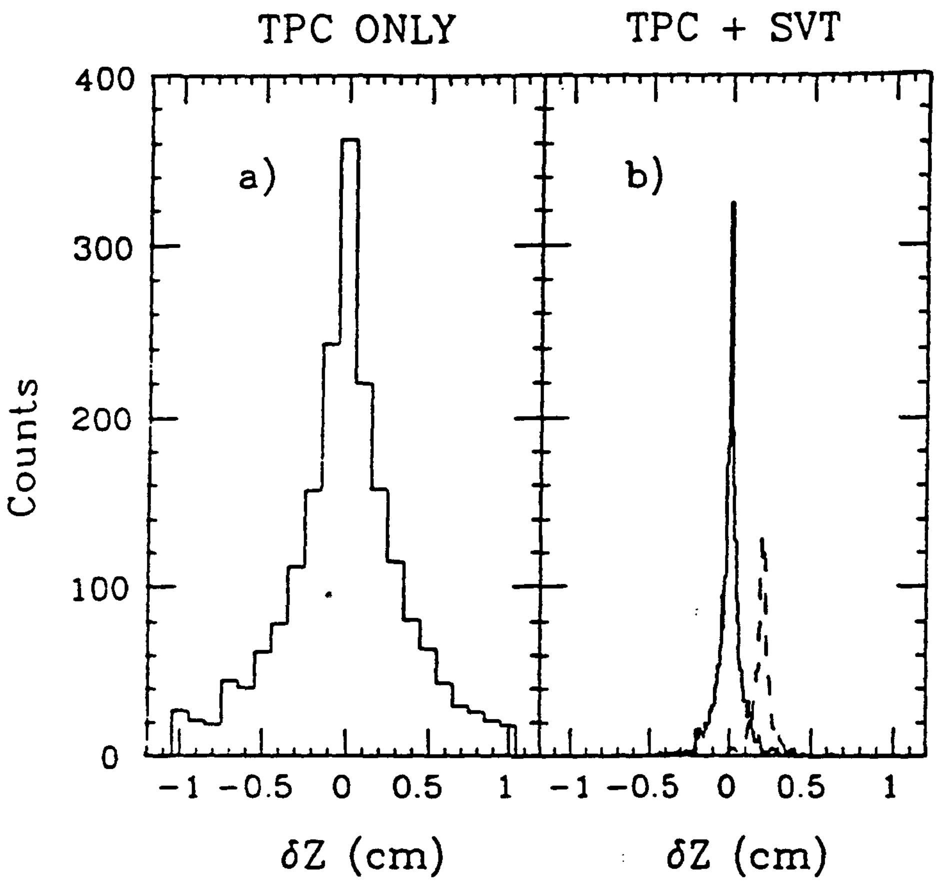

Fig.3 Primary vertex resolution (along beam direction) using: TPC tracking only (a) and TPC+ SVT tracking(b).

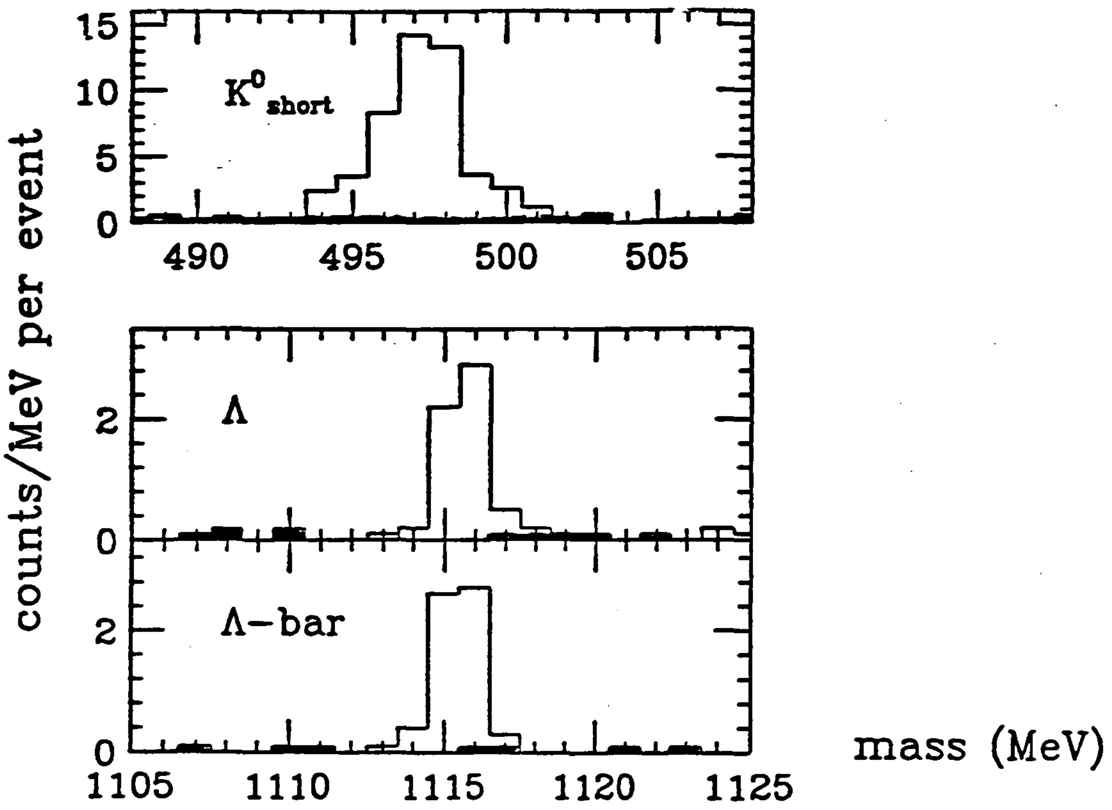

Fig.4 Invariant mass plots for Λ, Λ and K^0 reconstructed from 10 full FRITIOF/GEANT Au+Au events. Shaded areas represent the contribution from random background.

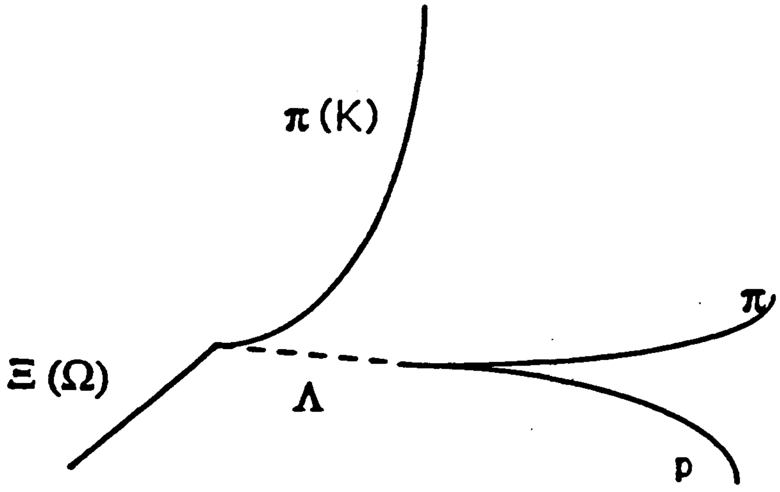

Fig.5 Topology for Ξ and Ω decays.

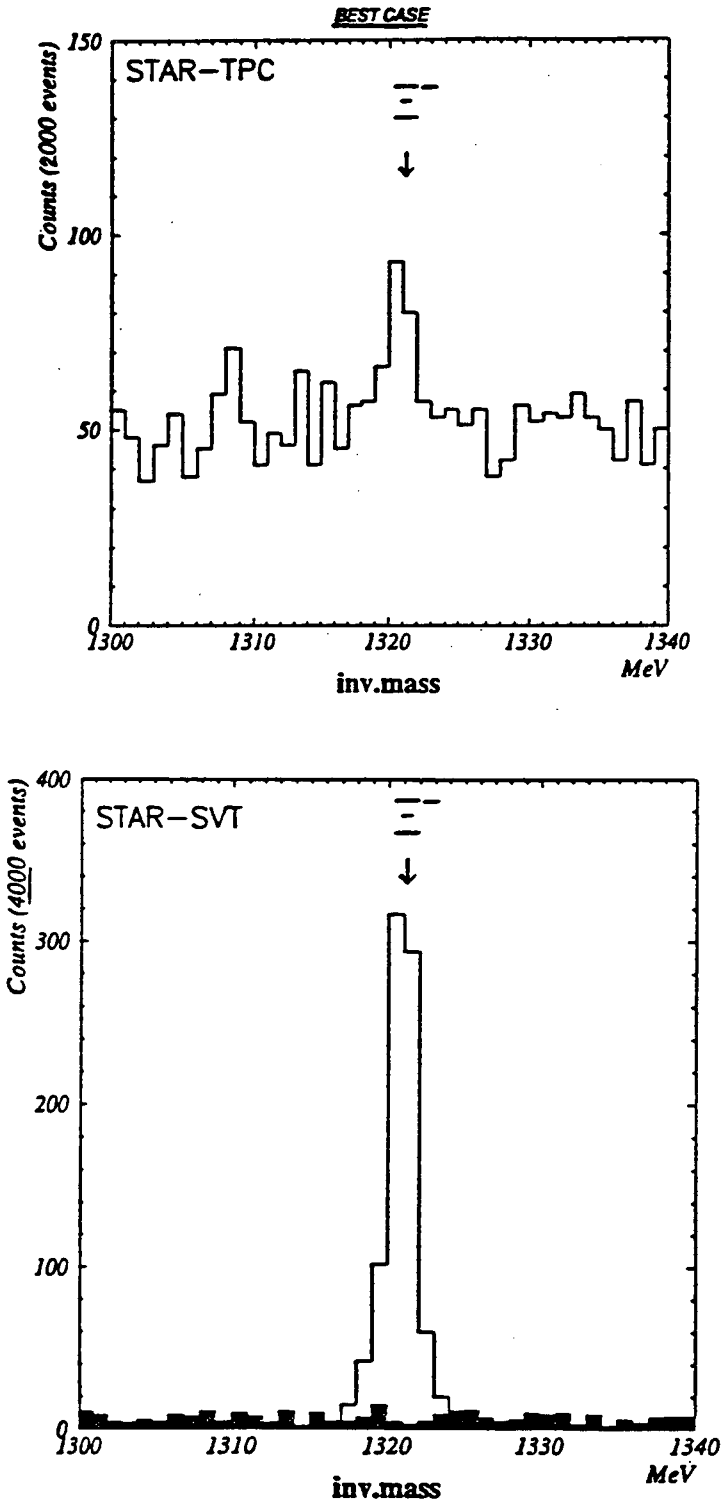

Fig.6 Invariant mass distributions ('ideal' case) for Ξ's reconstructed in STAR TPC (a) alone and TPC with the SVT (b). Shaded areas represent the contribution from random background.

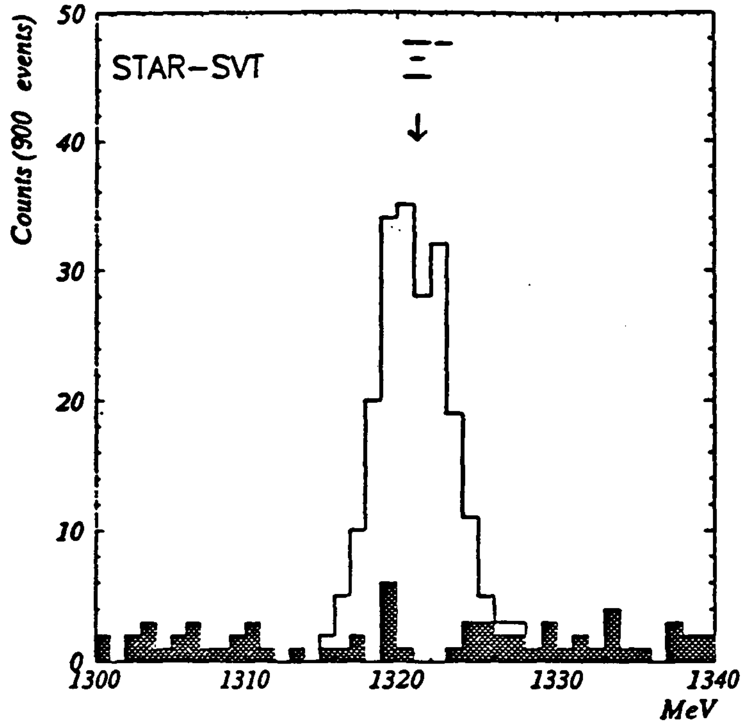

Fig.7 Invariant mass distribution of Ξ (TPC+SVT) with TPC momentum resolution taken to the account. Shaded areas represent the contribution from random background.

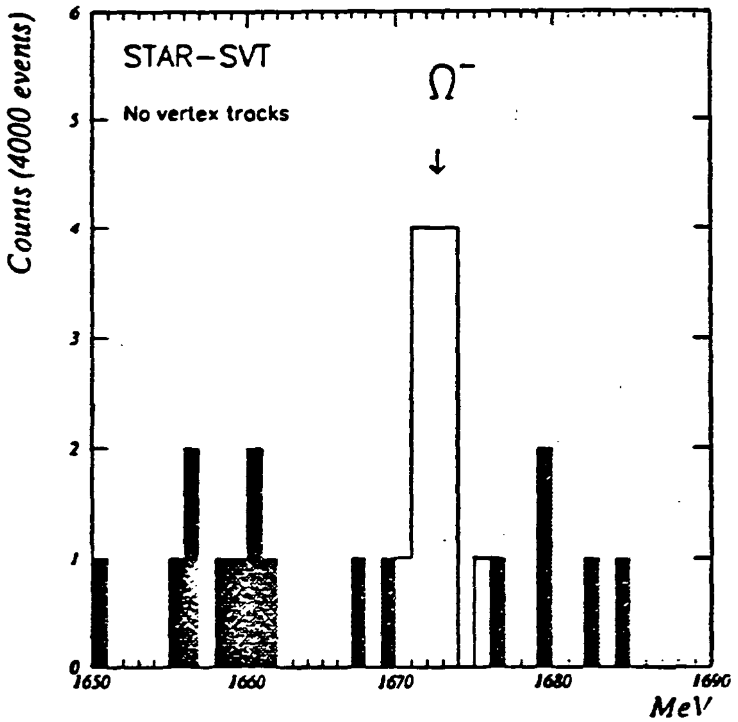

Fig.8 Invariant mass distribution of Ω reconstructed in STAR SVT and TPC. Shaded areas represent the contribution from random background.

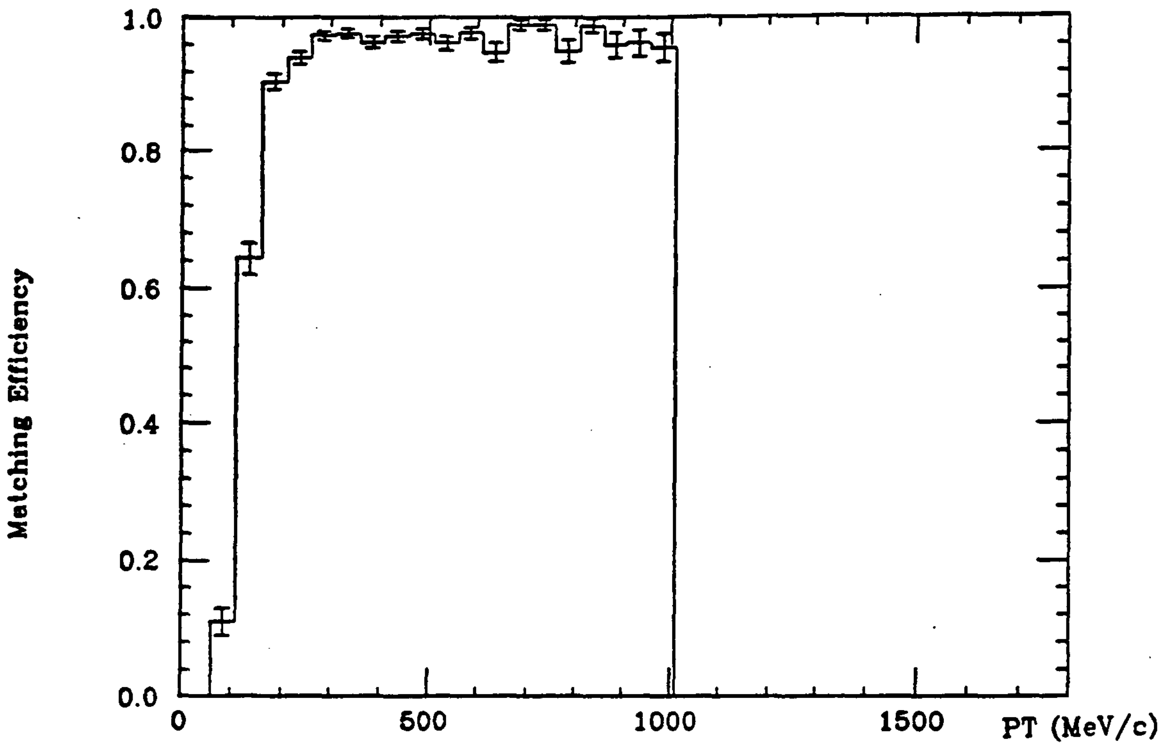

Fig.9 Matching efficiency as a function of pt.

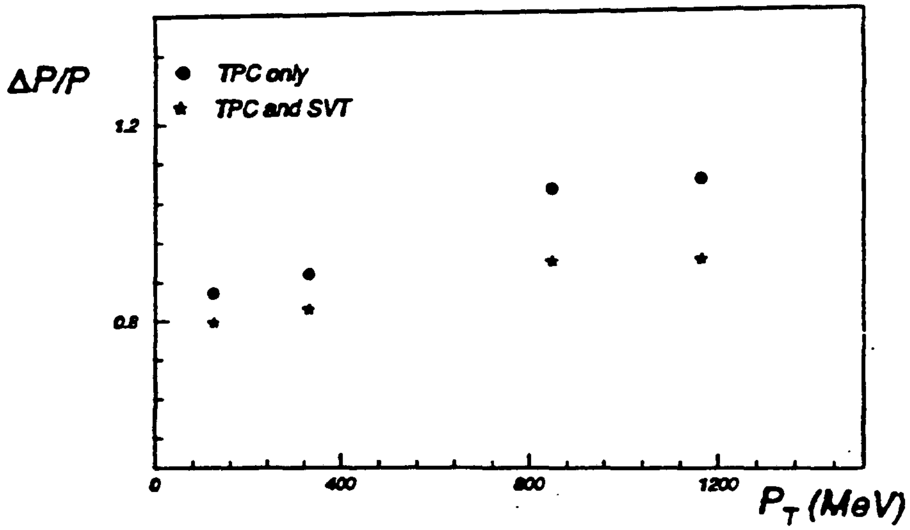

Fig.10 Momentum resolution for tracks reconstructed by TPC hits alone and by TPC hits and SVT hits. The same track sample has been used to derive these numbers.

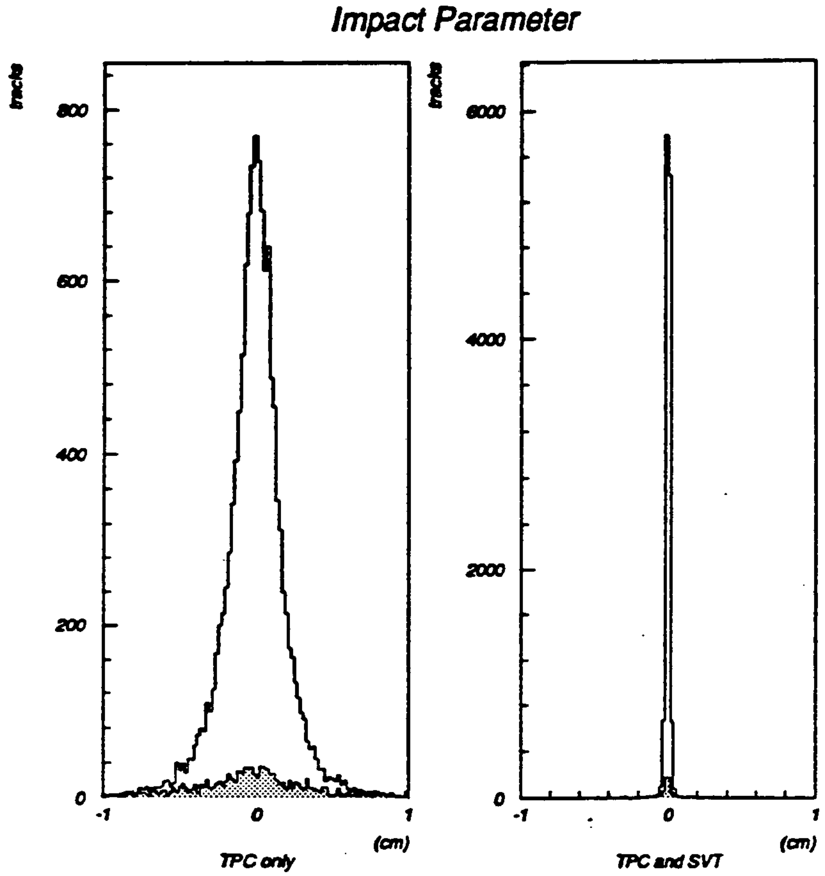

Fig.11 Impact parameter distribution of reconstructed primary tracks. For comparison the impact parameter distribution of secondary tracks is shown in the shaded area.

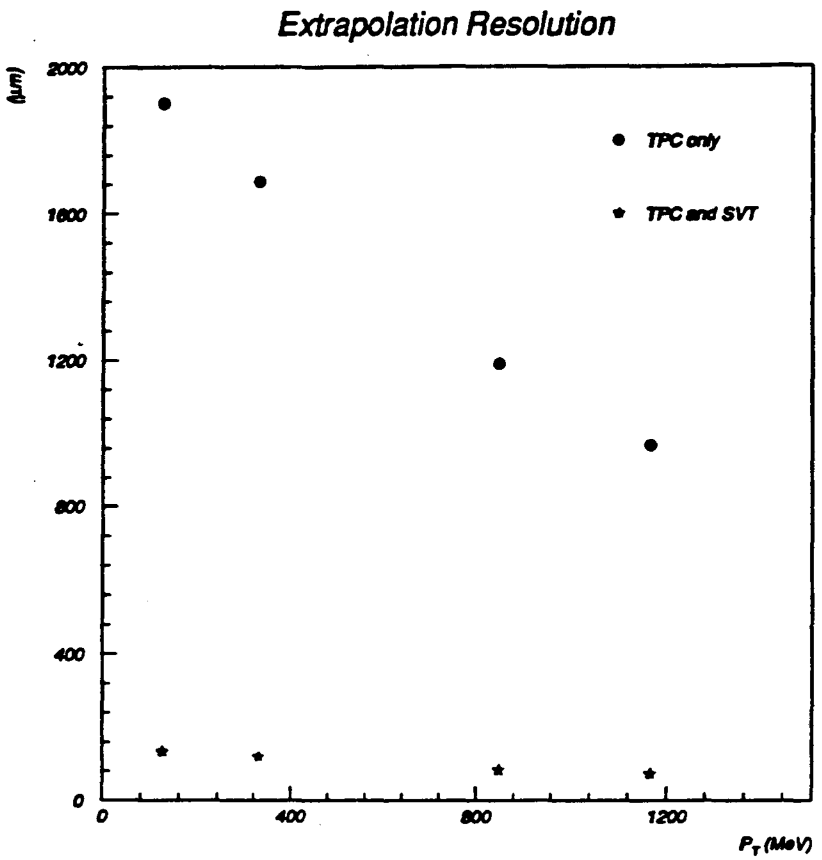

Fig.12 Extrapolation resolution to the vertex region for tracks reconstructed by TPC hits alone and by TPC hits and SVT hits. The same track sample has been used to derive these numbers.

LAWRENCE BERKELEY LABORATORY
UNIVERSITY OF CALIFORNIA
INFORMATION RESOURCES DEPARTMENT
BERKELEY, CALIFORNIA 94720